Bibliographical reference

Aircraft Noise: New Aspects on Lateral Sound Attenuation, W. Krebs and G. Thomann, Acta Acustica **vol. 95** (Number 6), 2009, pp. 1013-1023

DOI
https://doi.org/10.3813/AAA.918233

ACTA ACUSTICA UNITED WITH ACUSTICA
Vol. 95 (2009) 1013 – 1023

DOI 10.3813/AAA.918233

Aircraft Noise: New Aspects on Lateral Sound Attenuation

W. Krebs, G. Thomann
Empa, Swiss Federal Laboratories for Materials Testing and Research, Laboratory of Acoustics, Ueberlandstrasse 129, 8600 Dübendorf, Switzerland. Walter.Krebs@empa.ch

Summary
The lateral attenuation of sound for different aircraft was investigated with the help of a spectral three-dimensional model of the sound source. This model allows an independent analysis of the directivity of the sound source and the attenuation due to sound propagation, including ground effects. The sound immission at lateral receiver points has been calculated for different geometries and for hard and soft ground. Sound levels calculated with the three-dimensional model were compared with corresponding values resulting by the rotationally symmetric model implemented in Flula2. The differences arising from the two models were applied in a comparison of the sound directivity of six different aircraft with the engine installation corrections proposed in the revised Doc 29 3rd edition. For aircraft with fuselage-mounted engines good agreement was found between our results and the proposed engine installation corrections. Poor agreement was observed only for aircraft with wing-mounted engines. Moreover our results suggest that the lateral directivity may differ even for aircraft with identical engine configurations. In the second part of the paper the overall influence of the ground effect on A-weighted sound levels is analysed. Results for different receiver heights and ground impedances are presented.

PACS no. 43.50.Lj

1. Introduction

Exact modelling of sound emission for individual aircraft is essential for accurate prediction of aircraft noise by means of computer simulations. In order to carry out reliable aircraft noise calculations both the sound source and the sound propagation have to be modelled as accurately as possible. Aside from the sound power of an individual aircraft the directivity of the sound source is of utmost importance. The composition of the sound source due to different partial sources and dynamic effects cause distinctive differences in the sound power radiated in the forward and backward direction of the moving aircraft. Differences exceeding 10 decibels are common for sound levels measured in different longitudinal directions relative to the direction of flight. In addition differences of the sound energy radiated in lateral directions may be caused by reflections and shielding. Although the longitudinal directivity of the sound radiated by aircraft in flight is much more pronounced than the lateral directivity, the impact on the resulting noise immission is limited in most cases. Due to the varying angle between the flight direction and the direction from the aircraft to the observer during a fly-by the effect of the longitudinal directivity is smeared to some extent. On the other hand the lateral directivity directly affects the resulting sound immission on the ground. Hence exact modelling of the lateral directivity is extremely important.

Up to now only few computer models have been able to reproduce the lateral directivity properly. In the absence of valid data most current aircraft noise simulation programs still have to rely on simplified methods to describe the sound impact of aircraft traffic, assuming a rotationally symmetric sound emission.

Recent studies revealed that this assumption is not valid for all aircraft types. Measurements taken at Logan airport [1] and at the Wallops Flight Facility [2] indicate that the lateral sound directivity depends on the engine configuration of the aircraft. Based on these results the SAE subgroup A-21 initiated a revision of SAE-AIR-1751 [3] concerning lateral attenuation. Engine installation corrections have been proposed for fixed-wing aircraft in SAE-AIR-5662 [4] superseding [5]. This methodology has also been adapted in the revised Doc 29 3rd edition [6]. Two different lateral directivities are assumed for aircraft with engines mounted beneath the wings and those with engines mounted at the fuselage. Similar measurements have been performed at Gardermoen airport at Oslo leading to somewhat different results [7].

In order to depict the three-dimensional sound directivity of different aircraft a detailed source model was developed at Empa [8]. This source model defines the spectral sound level at a reference distance on a sphere by means of spherical harmonics. Based on acoustic measurements taken from real aircraft traffic the sound directivity of six

Received 22 April 2009,
accepted 13 July 2009.

fixed-wing aircraft was established. The analysis of data and the resulting directivity characteristics are presented in [9]. In the present paper we investigate the effects of the three-dimensional directivity of the sound source with respect to the resulting noise levels at sideline receivers. Furthermore the influence of the ground effect for different receiver heights and ground surfaces is calculated and compared to existing correction functions for lateral attenuation.

2. Context

The sound power generated by a sound source at the receiver position is dominated by two major factors:

1. the sound power of the sound source, including directivity,
2. sound propagation from the source to the receiver.

These factors have to be considered adequately by simulation models in order to reproduce the sound immission realistically.

Sound propagation in the atmosphere and ground effects have been well explored in the field of acoustics in the last decades. An analytical method of calculating the attenuation of sound as a result of atmospheric absorption is specified in the ISO Standard ISO 9613-1 [10]. The attenuation is given as a function of the frequency of the sound and the temperature, humidity and air pressure for a variety of meteorological conditions.

In addition to atmospheric attenuation, sound propagation is significantly affected by the acoustic properties of the ground. The sound field from a point source in air above an impedance plane was originally studied by Ingard [11], Lawhead and Rudnick [12] and later by Chien and Soroka [13] and in a number of subsequent studies, i.e.[14] [15].

The core issue in applying these results is the requirement of knowing the acoustic impedance of the ground. A widely used single-parameter model for the acoustic impedance described by the flow resistivity was proposed by Delany and Bazley [16]. Chessel [17] showed that this theory agreed well with experimental measurements over grass-covered surfaces. More comprehensive models were proposed to account for the porosity of the ground [18] and to make allowance for mixed impedance surfaces [19] [20].

The sound field above an impedance plane is also affected by the nature of the sound source. Li *et al.* [21] have shown that the sound field from a dipole above an impedance plane differs from that due to a monopole above this plane. Effects due to moving sources have been studied by Li *et al.* [22] and Buret *et al.* [23]. However the predicted effects on the ground attenuation are rather small. Pronounced effects on sound propagation arise due to inhomogeneous atmospheric conditions. In particular, atmospheric refraction caused by vertical gradients of temperature and wind influences the received sound pressure levels at large propagation distances [24]. However, due to the complexity of these effects and due to the lack of comprehensive source data current aircraft noise calculation programs do not make use of these features to the full extent. Different techniques are used to calculate the sound immission at a receiver point. A very efficient procedure is given in SAE-AIR 1845 [25]. According to [25] the sound immission at the receiver is defined by sound power distance tables (NPD) where the complete sound exposure level resulting for an entire flyover is predefined for different thrust settings and distances. The atmospheric attenuation is included in this description in an integrated way. Appropriate adjustments have to be applied to calculate the sound immission for non-standard conditions, i.e. for curved flights or specific atmospheric conditions. It is obvious that the possibilities provided by this method are limited. The Integrated Noise Model INM [26], developed by FAA, is based on this method.

A different approach is used in the aircraft noise simulation program Flula2 [27]. In Flula2 the sound source of different aircraft is defined by a mathematical model describing the A- weighted sound level as a function of the distance between the sound source and the receiver and as a function of the emission angle relative to the flight path. The model is assumed to have rotational symmetry in the axis of flight. The atmospheric attenuation is included in this description of the sound source. The coefficients of the model are fitted to acoustic measurements taken on the aircraft in flight. A time-step model of discrete sound sources along the flight trajectory yields the resulting immission levels. No restrictions arise due to complex flight geometries or hilly topography.

Another description of the sound source is used in the German models AzB [28] and DIN 45'684-1 [29]. In these models the sound source is defined by the spectral sound pressure levels at a fixed distance (AzB) or the spectral sound power (DIN). The sound propagation in the atmosphere can be calculated independently of the sound source.

3. Lateral attenuation

Aircraft noise calculation programs use empirically derived correction functions to take into account effects for slant sound incidence, often called lateral attenuation. Lateral attenuation is the reduction of the sound level to the side of the aircraft compared to the sound level measured below the aircraft at the same distance. It is a combination of three different physical effects,

1. ground effects, i.e. interference between directly radiated sound and the sound reflected from the surface,
2. attenuation by refraction and scattering caused by wind and meteorological conditions, generating e.g. shadow zones,
3. engine installation effects.

A generic method for modelling lateral attenuation was published by the Society of Automotive Engineers (SAE) in AIR- 1751 [4] in 1981. This method is based on experimental data on sound propagation from aircraft with

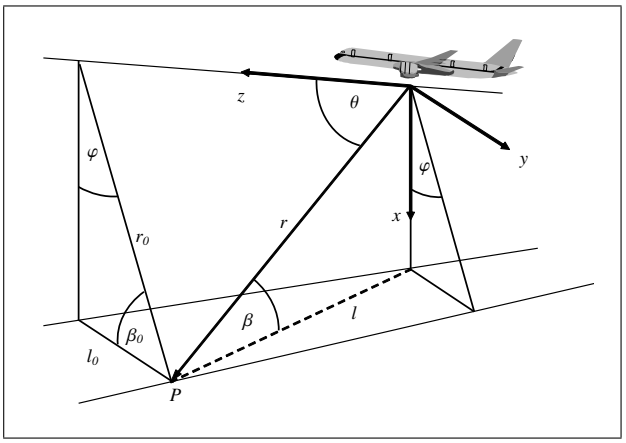

Figure 1. Schematic representation of the coordinate system and the notation used in this paper.

fuselage-mounted engines in straight level flight. According to this method lateral attenuation can be defined by

$$\Lambda(\beta_0, l_0) = G(l_0)\Lambda(\beta_0) \quad [\mathrm{dB}], \tag{1}$$

with
$$G(l_0) = 1.089[1 - \exp(-0.00274 l_0)] \quad \text{for } 0 \le l_0 \le 914\,\mathrm{m}(3000\,\mathrm{ft}),$$
$$G(l_0) = 0 \quad \text{for } l_0 > 914\,\mathrm{m},$$
$$\Lambda(\beta_0) = 3.96 - 0.066\beta_0 + 9.9\exp(-0.13\beta_0) \quad \text{for } 0° \le \beta_0 < 60°,$$
$$\Lambda(\beta_0) = 0 \quad \text{for } 60° \le \beta_0 \le 90°.$$

β_0 is the angle of sound incidence at the receiver P relative to the horizontal plane at the closest point of approach between flight trajectory and receiver, l_0 is the horizontal distance between the ground track and the receiver at the point of closest approach (see Figure 1)

Similar but slightly different formulas for lateral sound attenuation are used in the aircraft noise simulation programs Flula2 [30] and AzB [28]. While the limiting angle according to AIR-1751 is 60°, the correction for lateral attenuation in AzB and Flula2 is limited to elevation angles not exceeding 15°. In Flula2 the following sound attenuation for small incidence angles applies [30],

$$\lambda(\beta, r) = \left[1 - 3.8637\sin\beta\right] \cdot \left[10.1451 - 9.9\exp(-0.00134 r)\right] \quad \text{for } \beta < 15, \tag{2}$$
$$\lambda(\beta, r) = 0 \quad \text{for } \beta \ge 15.$$

The methodology used in AzB [28] depends on the spectrum of the sound source and yields similar values for the attenuation for small incidence angles. The formula for the sound level attenuation of the octave band n is

$$\Lambda_n(\beta_0, r) = (1 - 3.8637\sin\beta_0)\frac{G_n R_n r_0/r_1}{\sqrt{1 + (R_n r_0/r_1)^2}}, \tag{3}$$

R_n: spectral directivity factor of the octave band n, G_n: asymptotic sound attenuation of the octave band n.

Note that in Equations (1) and (3) the sound incidence angle β_0 at the closest point of approach applies while in equation (2) the varying sound incidence angle β for the actual source receiver geometry during the entire flyover is employed.

Recent studies [1] [2] [3] [7] have shown that lateral attenuation is affected significantly by the engine configuration of the aircraft and that equation (1) does not hold for all aircraft types. For this reason the SAE A-21 committee on aircraft noise initiated a revision of the lateral attenuation prediction methodology. A modified method is proposed in SAE-AIR-5662 [5]. This methodology has also been adopted in the revised Doc29 [6]. According to this method engine installation effects are considered explicitly for different aircraft configurations. As a consequence the lateral attenuation is separated into two terms,

$$\Lambda(l_0, \beta_0, \varphi) = A_{Grd+RS}(l_0, \beta_0) - E_{Eng}(\varphi), \tag{4}$$

with $A_{Grd+RS}(l_0, \beta_0)$: Attenuation due to ground and refraction/scattering effects, $E_{Eng}(\varphi)$: Engine installation effects.

The engine installation effects for aircraft with fuselage mounted-engines (E_f), wing-mounted engines (E_w) and for propeller aircraft (E_p) are given by the following expressions [6]:

$$E_f(\varphi) = 10\lg(0.1225\cos^2\varphi + \sin^2\varphi)^{0.329}, \tag{5a}$$
$$E_w(\varphi) = 10\lg\frac{(0.00384\cos^2\varphi + \sin^2\varphi)^{0.062}}{(0.8786\cos^2 2\varphi + \sin^2 2\varphi)}, \tag{5b}$$
$$E_p(\varphi) = 0. \tag{5c}$$

Recognising that the attenuation equation given in AIR 1751: 1981 [4] (see equation 1) holds reasonably well for aircraft with fuselage-mounted jet engines, an expression for the attenuation by ground and refracting-scattering effects can be determined by subtracting the engine-installation effect given by equation (5a) from the attenuation expression given in equation (1). For practical reasons this difference is approximated by the following relationship [5] [6]:

$$A_{Grd+RS}(\beta_0, l_0) = G(l_0)\Lambda(\beta_0) \quad [\mathrm{dB}], \text{ with} \tag{6}$$
$$G(l_0) = 1.089[1 - \exp(-0.00274 l_0)] \quad \text{for } 0 \le l_0 \le 914\,\mathrm{m}(3000\,\mathrm{ft}),$$
$$G(l_0) = 0 \quad \text{for } l_0 > 914\,\mathrm{m},$$
$$\Lambda(\beta_0) = 1.137 - 0.0229\beta_0 + 9.72\exp(-0.142\beta_0) \quad \text{for } 0° \le \beta_0 < 50°,$$
$$\Lambda(\beta_0) = 0 \quad \text{for } 50° \le \beta_0 \le 90°.$$

The lateral attenuation according to the four models described above is indicated in Figure 2. The diagrams show the resulting sound attenuation as a function of the (horizontal) distance l_0 between the observer and the ground track for three different incidence angles β_0. The height of the receiver above ground is not explicitly taken into account in these models.

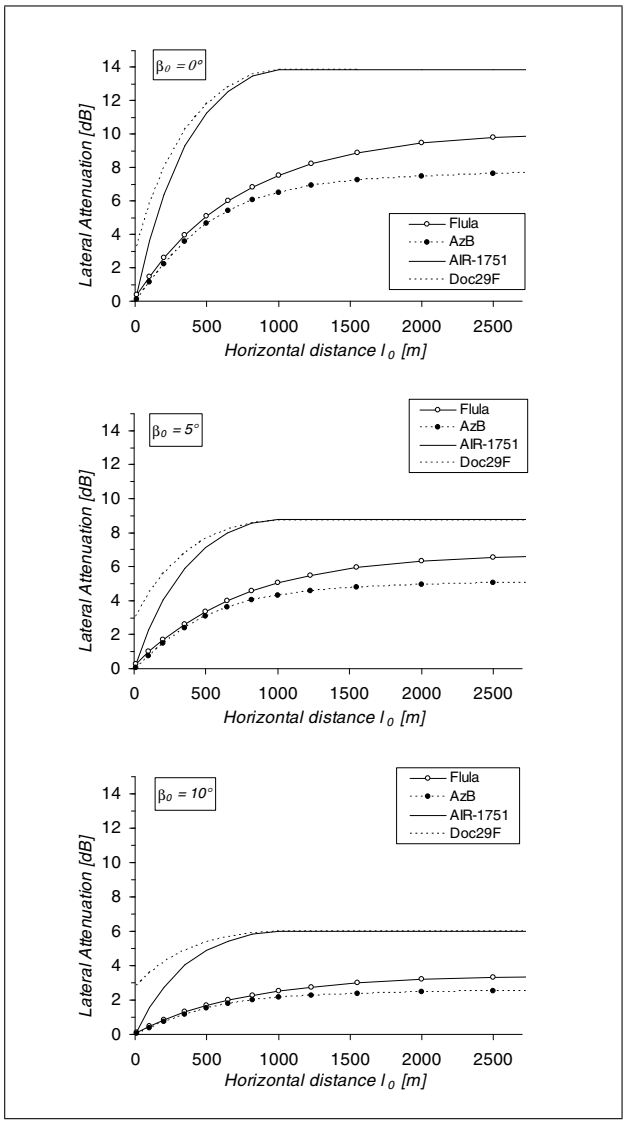

Figure 2. Attenuation of the A-weighted sound level at small angles of incidence as a function of the horizontal distance l_0 between the ground track and the receiver. The diagrams show the attenuation according to the formulas implemented in the aircraft noise simulation programs Flula2 and AzB and the corrections given in SAE-AIR-1751 and Doc29 3rd edition for aircraft with fuselage-mounted engines. The three diagrams represent the attenuation resulting for the three incidence angles $\beta_0 = 0°$, 5° and 10°.

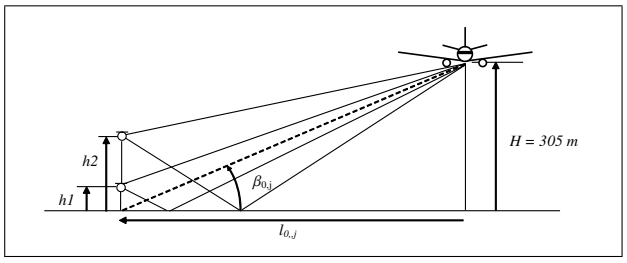

Figure 3. Geometric layout of the simulation.

For very small incidence angles below 2 degrees large discrepancies up to 7 decibels arise between the corrections resulting from the different models. For moderate incidence angles in the range 10°...30°and distances from 300 m up to 3000 m differences from 2 to 4 decibel arise. A comparison of the models shows that the method used to account for lateral attenuation significantly affects the sound level calculated at lateral positions and hence affects the extension of the resulting noise contour. Therefore detailed knowledge of the appropriate attenuation is of utmost importance in order to perform reliable numeric simulations.

With help of the new spectral three-dimensional sound directivity models developed at Empa [8] [9] the influence of the different effects involved in lateral attenuation can be studied in detail. First results of these studies are presented in the next sections.

4. Design of the investigation

The sound propagation was investigated using a three-dimensional spectral source model. This model defines the spectral sound pressure level $L_k(\theta, \varphi)$ at the reference distance r_{ref} of 305 m in the direction (θ, φ) for standard atmospheric conditions. The geometric notation used is given in Figure 1. With this source model the sound exposure level was calculated at several immission points for individual flyovers and compared to the sound exposure levels calculated with the rotationally symmetric model of Flula2 for the same aircraft type. Since the three-dimensional model and the rotationally symmetric model of Flula2 are both based on the identical acoustic measurements [9] [10], the resulting differences are a direct measure of the influence of the lateral directivity of the sound source and on effects due to different implementations in the three-dimensional model and in the rotationally symmetric model of Flula2 to account for effects at slant incidence angles.

We used a simple design in order to facilitate the analysis and interpretation of the results. The A-weighted sound level was calculated for a straight level flight at constant speed and constant height $H = 305$ m at several immission points located in a line perpendicular to the flight path (see Figure 3). The geometric parameters of the immission points are given in Table I. For each immission point calculations were performed for two different receiver heights h_1 and h_2. In order to facilitate the interpretation of the results the sound incidence angles $\beta_{0,j}$ used in the following discussion refer to the ground line of the receivers. However in the calculations the real geometric conditions were properly considered in regard to the actual receiver height including the sound propagation path reflected on the ground.

The complete time history of the sound level at the receiver points is calculated using a time-step method with a time increment of 1 second. For each emission point the sound level resulting at the immission points is calculated with the three-dimensional source model and with the rotationally symmetric model considering the following effects:

1. directivity of the sound source,
2. geometric spreading,
3. atmospheric attenuation,
4. ground effect (three-dimensional model) or sound attenuation for small incidence angles (rotationally symmetric model).

Constraints:

The sound source is placed at discrete positions along the flight trajectory. Effects due to source motion related to sound propagation and ground effect are not considered explicitly. However Doppler shift is included implicitly in the spectral directivity model of the sound source to account for the derivation of the model from real measurements [31].

According to this procedure each emission point i generates the A-weighted sound level $L_{A,i,3d}$ for the three-dimensional model and $L_{A,i,rs}$ for the rotationally symmetric model at the receiver,

$$L_{A,i,3d} = 10\lg\left(\sum_{k=1}^{m} 10^{(L_k(r_{ref},\theta_i,\varphi_i)-20\lg(r_i/r_{ref}))/10} \cdot 10^{(-\alpha_k(r_i-r_{ref})+g_k(r_i,\beta_i,h,\sigma)+\Delta_k)/10}\right), \quad (7)$$

with $L_k(r_{ref}, \theta_i, \varphi_i)$: Sound pressure level for the one third octave band k at reference distance r_{ref} in the direction (θ, φ), $g_k(r_i, \beta_i, h, \sigma)$: spectral ground effect for the one third octave band k [20], r_i: distance between sound source and observer for the emission point i, β_i: incidence angle at the observer for the emission point i, h: height of the receiver above ground, σ: flow resistance of the ground, α_k: sound attenuation coefficient at 15°C, 70% r.h. according to ISO 9613-1 [10], Δ_k constants for A-weighting [32].

The ground effect is calculated according to the impedance model of Delany and Bazley [16], where the acoustic impedance of the reflecting surface is parameterized by the flow resistivity of the ground. The sound level at the receiver was calculated by the coherent addition of the sound wave propagating directly from the source to the receiver and the wave reflected on the ground, using spherical wave reflection coefficients [20]. For the simulations a homogeneous, flat and local reacting surface was assumed. For each 1/3 octave frequency band the energetically averaged mean value was calculated by integrating over the appropriate frequency range.

For the rotationally symmetric model the A-weighted sound level is given by

$$L_{A,i,rs} = L_A(r_i, \theta_i) - \lambda(r_i, \beta_i), \quad (8)$$

with $L_A(r_i, \theta_i)$: A-weighted sound level at the distance r_i in the direction θ_i. Geometrical spreading and air absorption for standard atmosphere are included in this model [31] [30], $\lambda(r_i, \beta_i)$: Sound attenuation for small incidence angles according to equation (2).

Table I. Horizontal distance to the flight track ($l_{0,j}$) and elevation angle $\beta_{0,j}$ of the immission points j.

j	$l_{0,j}$ [m]	$\beta_{0,j}$
1	0.0	90°
2	53.8	80°
3	111.0	70°
4	176.1	60°
5	255.9	50°
6	363.5	40°
7	528.3	30°
8	838.0	20°
9	1138.3	15°
10	1729.7	10°
11	3486.2	5°

Table II. Summary of aircraft types analysed. Legend: Type - Short name. Aircraft - Aircraft type. Config. - Engine configuration: J2W: 2 wing-mounted turbofans, J2F: 2 fuselage-mounted turbofans, J3W/F: 3 turbofans, 2 wing-mounted plus 1 fuselage-mounted, J4W: 4 wing-mounted turbofans, T2: 2 turboprops. Eng. - Engine installation effect according to Doc 29 3rd edition. N - Numbers of flyovers measured, used in model definition.

Type	Aircraft	Config.	Eng.	N
A3103	Airbus A310-300	J2W	Ew	7
A320	Airbus A320	J2W	Ew	22
MD11	McDonnell Doug. MD-11	J3W/F	Ew	8
MD83	McDonnell Doug. MD-83	J2F	Ef	10
RJ100	BAe Avro RJ-100	J4W	Ew	33
SB20	Saab 2000	T2	Ep	20

Knowing the instantaneous sound levels L_{Ai} the sound exposure level L_{AE} is calculated using the fixed time interval $\Delta T = 1$ second.

$$L_{AE} = 10\lg\left(\frac{1}{T}\sum_{i=0}^{n} 10^{L_{Ai}/10} \cdot \Delta T\right). \quad (9)$$

The sound exposure level $L_{AE,3d}$ is calculated for a complete flyover for each immission point given in Table I. Three-dimensional source data for 6 different aircraft are available [9]. A summary of the characteristics of these aircraft is given in Table II. Calculations were performed for two receiver heights $h = 1.2$ m and $h = 10$ m for hard and soft ground.

In order to assess and quantify the effects of the lateral directivity of the sound source we compared the sound exposure levels calculated with the three-dimensional spectral model with the sound exposure levels calculated with the standard source data of Flula2, i.e. the rotationally symmetric model.

5. Comparison of the sound exposure levels

The sound exposure levels were calculated with the three-dimensional model ($L_{AE,3d}$) and with the rotationally symmetric model of Flula2 ($L_{AE,rs}$) for a straight level

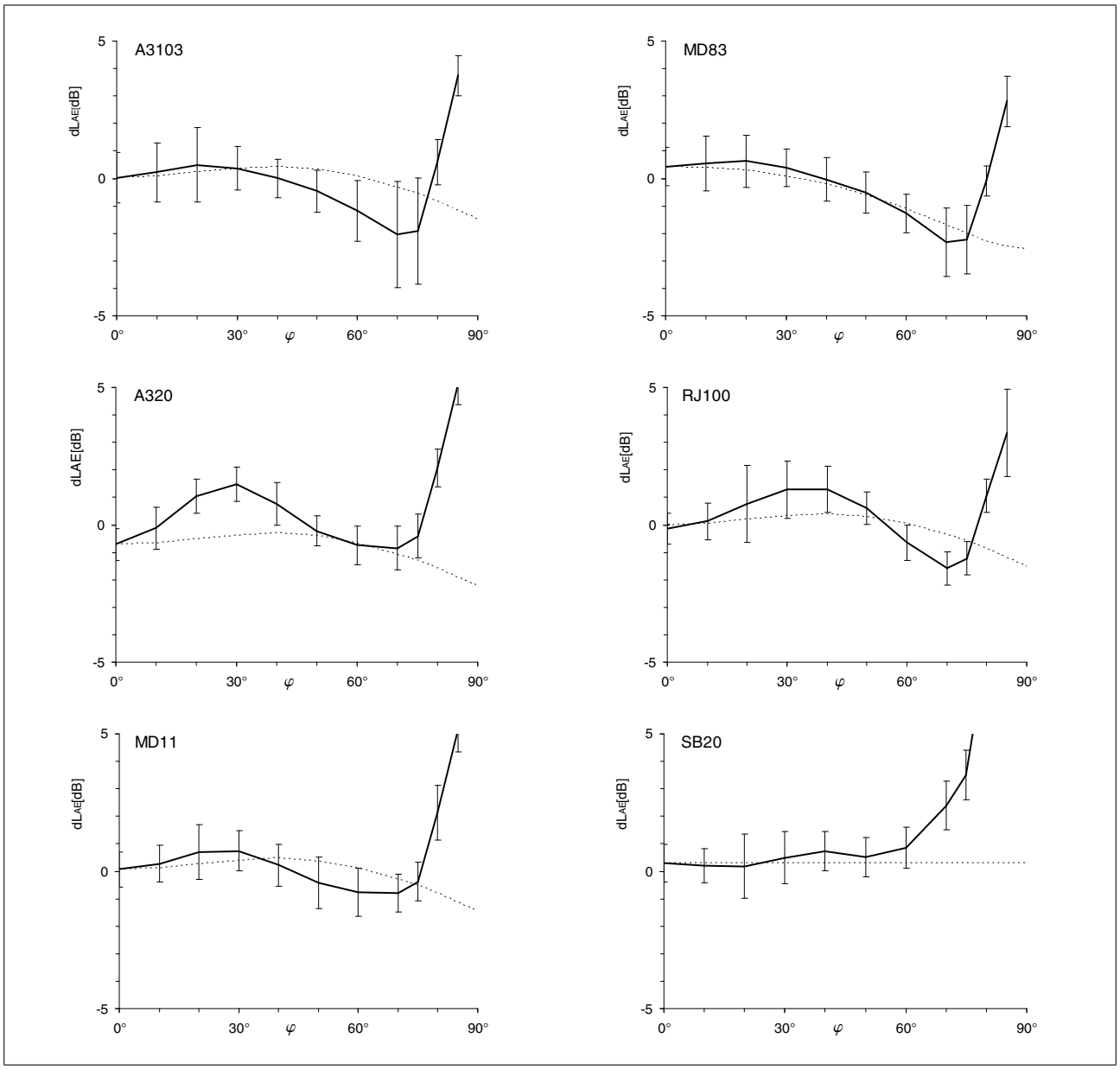

Figure 4. Lateral sound directivity for different aircraft. Solid line: Difference dL_{AE} between the A-weighted sound immission levels calculated with the three-dimensional model and with the rotationally symmetric model. Error bars show the standard uncertainty according to equation (10). Dashed line: Engine installation correction E_f, E_w, or E_p proposed in Doc29 for the corresponding aircraft type.

flight at a height $H = 305$ meters at the immission points given in Table I. The differences $dL_{AE} = L_{AE,3d} - L_{AE,rs}$ between the sound exposure levels calculated with the two models for the aircraft analysed are given in Figure 4. For comparison the engine installation correction given in Doc 29 3rd edition [6] for the corresponding aircraft types are indicated in the diagrams as well. Error bars indicate the uncertainty of the directivity according to our analysis. The resulting standard uncertainty of the three-dimensional source model is estimated by the following relation:

$$u_{3d} = \sqrt{\left(\frac{SD}{\sqrt{N}}\right)^2 + u_m^2}, \qquad (10)$$

with SD: Standard deviation of the measured A-weighted sound levels used to derive the three dimensional source model within a solid angle of 10°× 10° (see Figure 5), N: Number of events, i.e. number of independent flights measured contributing to the corresponding direction [31], u_m: Standard uncertainty of the measurements, estimated as 0.5 dB.

The uncertainty is predominated by the uncertainty of the fit of the model to the measured data and the uncertainty of the measured data itself. The uncertainty of the fit is estimated by the dispersion of the measured data used to derive the parameters of the three-dimensional model and normalised by the square root of the number of independent measured flights (see Figure 5). The sound expo-

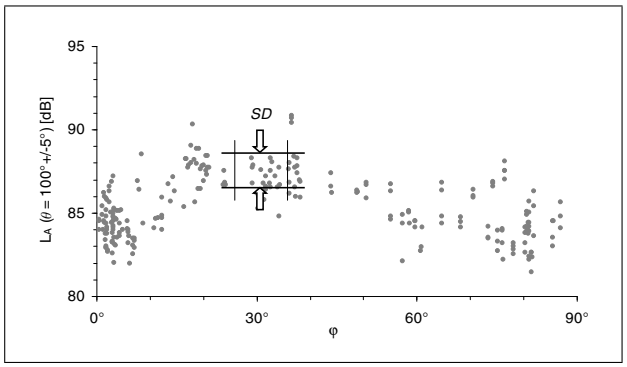

Figure 5. Schematic representation of the dispersion of the measured sound levels. Dots represent A-weighted sound levels, normalised to the reference distance $r_{ref} = 305$ meters in the interval of the polar angle with $95° \leq \theta \leq 105°$ as a function of the azimuth angle φ. The standard deviation SD of these sound levels is calculated for bins spaced by 10 degrees.

sure level for a complete flyover is predominated by the maximum sound level. Therefore the resulting uncertainty is estimated using the dispersion of the measured sound data corresponding to the emission angle of the maximum sound level. This emission angle is about 100 degrees for most aircraft analysed in this study. Hence emission angles θ with $95° \leq \theta \leq 105°$ were considered to estimate the standard deviation in equation (10). In order to estimate the decisive dispersion for the relevant azimuth angle the measured sound levels, normalised to the reference distance $r_{ref} = 305$ meters, were portioned into $10° \times 10°$ sized bins. The standard deviation SD was then calculated for each bin.

The deviations dL_{AE} between the sound levels calculated with the three-dimensional model with respect to the levels calculated with the rotational symmetric model originate from two different effects,

a) differences in sound level due to non-uniform lateral sound radiation of the source,
b) differences caused by different methods to account for sound attenuation effects at small incidence angles, i.e. at azimuth angles near 90 degrees.

The latter results in a general increase of the differences dL_{AE} at azimuth angles exceeding 70°; this is discussed in more detail in the next section. At lateral angles $\varphi \leq 70°$ the sound incidence angles are large for the relevant segment of the flight path; thus effects caused by ground effects are less important. The differences observed between the calculations with the two models are a consequence of the lateral directivity of the three-dimensional source model.

The analysis of the resulting sound exposure levels confirms our previous findings on the lateral directivity [9] to a large extent. A considerable variation of the sound exposure level with respect to the rotationally symmetric model is found for the aircraft A320 and RJ100. For both aircraft an increase of the sound level with respect to the rotationally symmetric model arises at lateral angles φ between 20 and 40 degrees. While the lateral variation of the resulting sound exposure level for the RJ100 is of the order of the uncertainty of the fitted model, a significant increase of the sound exposure level with respect to a rotational symmetric model is found for the Airbus A320. The variation of the sound exposure level with respect of the rotationally symmetric model is 2.2 dB at the lateral angle $\varphi = 30$ degrees, the uncertainty is estimated to be 0.6 dB.

This effect is not observed for the Airbus A310-300 in accordance with the findings in [9]. Although the configuration of this aircraft is the same as that of the A320, i.e. two wing-mounted turbofan engines, the lateral directivity of the A310-300 differs from the directivity found for the A320. The directivity found for the A310-300 is similar to the directivity of the MD83, which matches the engine installation correction according to Doc29 [6] for fuselage-mounted aircraft very well. For the MD83 the deviation between our calculations and Doc29's correction is less than 0.6 decibel for azimuth angles up to 70 degrees.

No clear evidence of a deviation from a rotationally symmetric directivity is found for the MD11 and the propeller-driven Saab 2000. The deviations of the sound levels with respect to the rotationally symmetric model are small, namely in the order of the estimated uncertainty.

6. Ground effects

At large azimuth angles, i.e. for small incidence angles, the exposure levels calculated with the three-dimensional model are generally higher than the levels calculated with the rotationally symmetric model (see Figure 4). Differences dL_{AE} up to 9 decibels are observed. This discrepancy arises mainly due to the different methods applied to account for sound attenuation at small incidence angles. The empirical formula used in Flula2 implies an additional attenuation for sound incidence angles below 15° (see equation 2). For small incidence angles this attenuation ranges up to 10 dB. On the other hand a spectral ground interference model is implemented in the three dimensional model (see section 4).

A detailed representation of the time history of the instantaneous sound level $L_{A,3d}$ together with the ground effect g_A for A-weighted sound levels according to the three-dimensional sound source model is given in Figure 6. Figure 6a applies to an immission point directly beneath the flight path and Figure 6b to an immission point located to the side at an azimuth angle of 75 degrees. At point a, the incidence angle increases from near zero to 90 degrees while the aircraft is flying along the trajectory. At point b, the immission angle starts at low values and culminates to $\beta_0 = 15$ degrees at the closest point of approach between the sound source and the receiver.

The diagrams in Figure 6 indicate that the ground effect for A-weighted sound levels g_A calculated according to [20], i.e. the difference between the A-weighted immission level and the corresponding sound level calculated without ground effect, varies only slightly during the "10 dB down" time interval, which is relevant for the total immission level L_{AE}. Although the ground effect calculated for

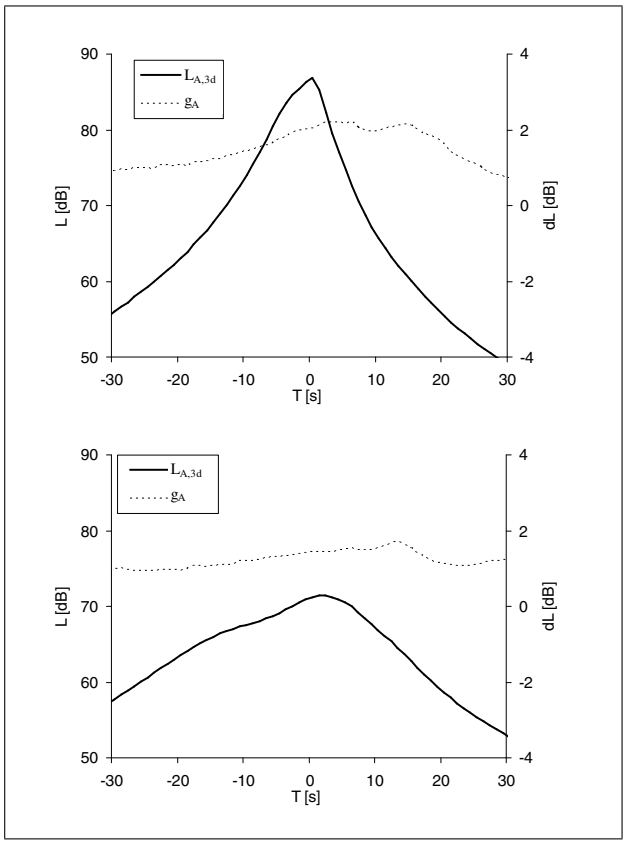

Figure 6. Time evolution of the A-weighted sound level calculated with the three-dimensional model for a flyover of an Airbus A320 at $H = 305$ meters and $v = 160$ kt at two different immission points at $h = 10$ meters and flow resisitivity $\sigma = 300\,\mathrm{kPas/m^2}$. Top: $\varphi = 0°$, bottom: $\varphi = 75°$. $L_{A,3d}$: A-weighted sound pressure level at the immission point according to equation (7). g_A: Ground effect for A-weighted sound levels (scale to the right).

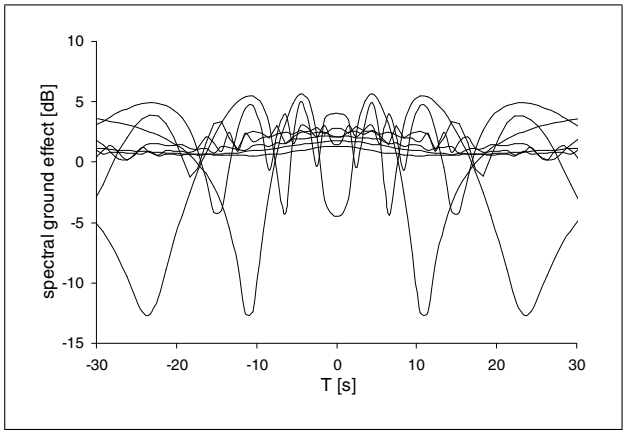

Figure 7. Example of the spectral ground effect for selected 1/3 octave bands in the frequency range from 25 Hz up to 2.5 kHz for the flyover shown in Figure 6a.

the individual 1/3 octave bands oscillates during the fly-by (see Figure 7), the resulting effect g_A is almost a constant and causes an increase of the free field sound level in the order of two decibels.

The overall impact of the ground effect G_A is assessed at each immission point by evaluating the difference between the A-weighted sound exposure levels calculated with ground effect minus the exposure levels calculated without ground effect for a complete fly-by.

$$G_A = L_{AE,3d,g} - L_{AE,3d,ng}, \tag{11}$$

with $L_{AE,3d,ng}$: Sound exposure level calculated without ground effect, $L_{AE,3d,g}$: Sound exposure level calculated with ground effect.

This calculation was performed for different aircraft types, for two different receiver heights and for two different ground impedances. The overall impact of the ground effect G_A with respect to the A-weighted exposure level is given in Figure 8. This representation shows that the overall effect G_A caused by the ground interference has a very similar shape for all aircraft powered by turbofan engines. The ground effect for A-weighted sound levels varies only slightly and smoothly with respect to the azimuth angle for these aircraft. A much more irregular behaviour of the ground effect arises for the Saab 2000; this is probably caused by tonal components contained in the spectra of propeller driven aircraft.

As expected the A-weighted ground effect is affected considerably by the ground impedance and the height of the receiver above ground. For soft ground ($300\,\mathrm{kPas/m^2}$) the resulting ground effect is about 2 decibels for incidence angles β_0 exceeding 30 degrees and is reduced smoothly towards small incidence angles. This reduction is more pronounced for a receiver at 1.2 meters above ground than for the receiver at 10 meters. Whereas for a receiver at 10 meters above ground the overall ground effect is reduced to +1 dB at low incidence angles, the effect is reduced down to 0 dB for receivers at 1.2 meters above ground.

In the case of hard ground a generally greater ground effect is observed (+2.8 dB). However in contrast to soft ground only a minor variation of the ground effect is observed with respect to the azimuth angle or incidence angle respectively. For the receiver at 10 meters above ground the ground effect for A-weighted sound levels is almost a constant value, independent of the incidence angle. For the receiver at 1.2 meters the overall ground effect remains constant for incidence angles above 20 degrees. After a minor decrease at $\beta_0 = 10$ degrees a considerable increase is found for very small incidence angles. No similar increase is observed when the receiver is placed at 10 meters above ground.

7. Discussion

Aircraft sound simulations have been carried out using a spectral three-dimensional sound source model. With this model the sound source is described independently of the sound propagation, therefore allowing detailed analysis of different effects which influence the resulting sound level at the receiver. As a result of the lateral directivity of the sound source a variation of the resulting exposure levels

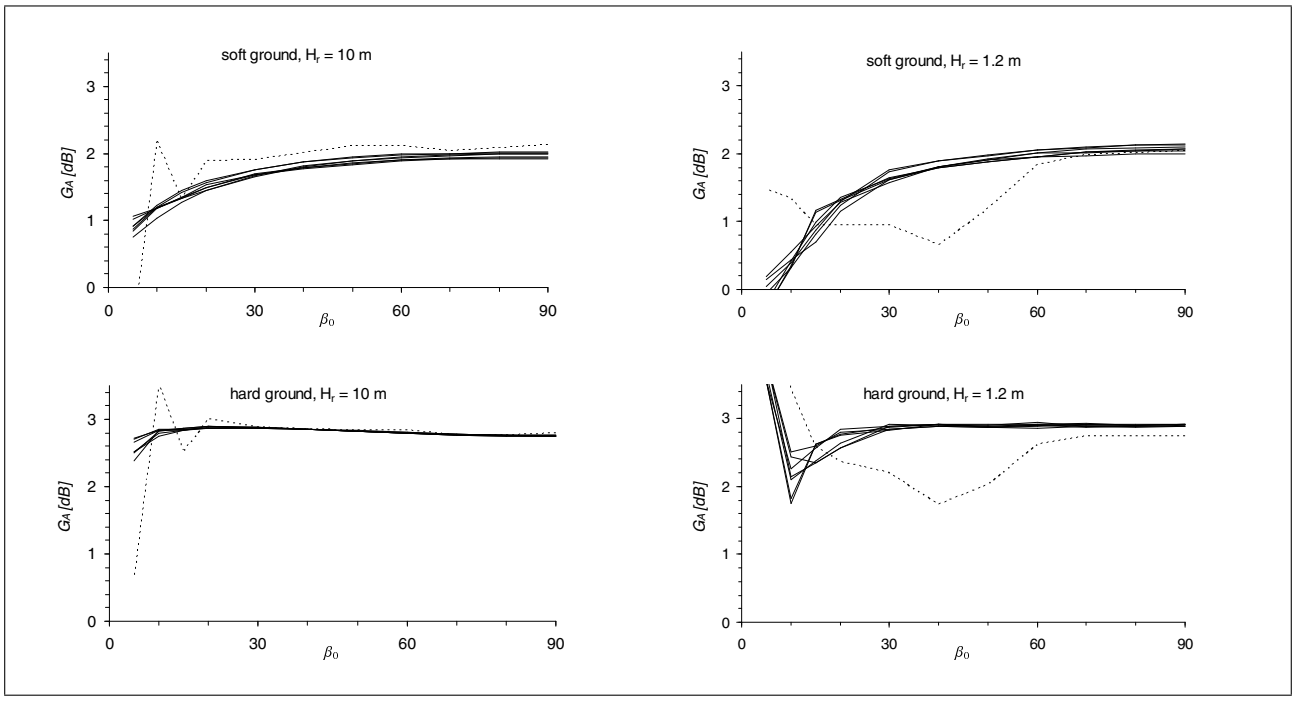

Figure 8. Overall impact of the ground effect G_A for different aircraft types according to the simulations with the three-dimensional source model. The lines represent the difference of the A-weighted sound exposure level L_{AE} calculated with the three-dimensional model including the spectral ground effect and calculations without ground effect. Solid lines: turbofan aircraft, dotted line: propeller driven aircraft (Saab 2000).

occurs with respect to calculations performed with a rotationally symmetric model based on the same acoustic measurements.

For aircraft with fuselage-mounted engines our findings agree well with the results of the Wallops Flight Facility Study [3] and the engine installation correction proposed in Doc 29 3rd edition [6]. A clear reduction of the sound power radiated in the horizontal plane with respect to the sound power measured below the aircraft is confirmed. In contrast to these findings considerable discrepancies arise between our results and the directivities reported in Doc 29 for aircraft with wing-mounted engines. The analysis with the three-dimensional model revealed that the lateral directivity may differ significantly even for aircraft with almost identical engine configuration. While the directivity observed for the Airbus A310-300 coincides to a large extent with the directivity reported for fuselage-mounted aircraft, the directivity established for the Airbus A320 matches neither the directivity for wing-mounted aircraft nor that for fuselage-mounted aircraft proposed in Doc 29. The increase of the sound levels for azimuth angles around 30 degrees is much more pronounced than the increase proposed by the engine installation correction for wing-mounted aircraft. The sole difference in the lateral directivity due to the engine configuration obviously does not hold for all aircraft types. Additional effects not characterised by the engine configuration may additionally affect the lateral directivity.

As a second result the definition of the sound source with the help of the spectral three-dimensional model enables a separate quantification of the overall impact of the ground effect with respect to the sound exposure level. Previous studies on the overall impact of the ground effect are mostly related to sound propagation near the ground with low source heights, which are appropriate for ground-to-ground propagation. For these situations large excess attenuations exceeding 10 decibels are found [23] [33]. On the other hand the source height is large for aircraft noise simulations and the findings for ground-to- ground propagation with respect to ground reflection and interference cannot be applied directly.

Our results show that for turbofan powered aircraft the overall impact of the ground effect on A-weighted sound exposure levels $G_A(l_0, \beta_0)$ depends only smoothly on the source-receiver geometry. Hence for these aircraft $G_A(l_0, \beta_0)$ could be modelled for a given ground impedance by a simple formula as a function of the sound incidence angle β_0 and the horizontal distance l_0 between the flight track and the receiver. In order to establish this relation additional simulations have to be performed exploring all relevant geometries between sound source and receiver.

In analogy to the procedure followed in SAE AIR 5662 [5], decomposing the lateral attenuation into two independent factors according to equation (4) for engine installation effects E_{Eng} and attenuation due to ground and refraction/scattering effects A_{grd+RS} the latter can be defined as

$$A_{grd+RS}(l_0, \beta_0) = A_{RS}(l_0, \beta_0) - G_A(l_0, \beta_0), \qquad (12)$$

with $A_{RS}(l_0, \beta_0)$: Attenuation due to refraction/scattering effects in the atmosphere, $G_A(l_0, \beta_0)$: Overall impact of the ground effect on A-weighted sound exposure levels.

The attenuation due to refraction/scattering in equation (12) can be evaluated by subtraction using the relation given in SAE AIR 5662 [5] for the combined ground and refraction/scattering effect A_{grd+RS}. According to this procedure the lateral attenuation, formerly represented in one single formulae is split into three independent elements. This will allow future simulation models to account for different sound propagation effects more easily.

The variation of the resulting sound exposure level due to effects caused by the spectral ground effect $G_A(l_0, \beta_0)$ is of the order of 1–2 decibels. This is only a small part of the total variation of the lateral attenuation, which is of the order of 10 decibels. This analysis reveals that the most important factor for the lateral attenuation is the meteorological term $A_{RS}(l_0, \beta_0)$. Therefore sophisticated and time consuming methods to evaluate the spectral ground effect do not contribute much to the accuracy and reliability of aircraft noise simulation programs designed to predict A-weighted sound levels. Future efforts to improve the overall performance of sound immission models should be focused on meteorological effects rather than on spectral ground effects.

Acknowledgement

We are grateful to our colleagues S. Pluess for accomplishing part of the simulations and K. Heutschi for his contributions to this work; we also thank A. Rosenheck for his linguistic revision of the manuscript.

References

[1] G. G. Fleming, D. A. Senzig, J.-P. B. Clarke: Lateral attenuation of aircraft sound levels over an acoustically hard water surface: Logan airport study. Noise Control Eng. J. **50** (2002) 19–29.

[2] A. Senzing, G. G. Fleming, K. P. Shepard: Measured engine installation effects of four civil transport airplanes. NoiseCon 2001, Portland, Maine, October 29-31, 2001.

[3] G. G. Fleming, D. A. Senzig, D. A. McCurdy, C. J. Roof, A. S. Rapoza: Engine installation effects of four civil transport airplanes: Wallops flight facility study. NASA/TM-2003-212433, National Aeronautics and Space Administration, Langley Research Center, Hampton, 2003.

[4] Society of Automotive Engineers, Committee A-21: Prediction method for lateral attenuation of airplane noise during takeoff and landing. SAE AIR 1751, 1981.

[5] Society of Automotive Engineers, Committee A21: Method of predicting lateral attenuation of airplane noise. SAE AIR 5662, superseding AIR 1751, 2005.

[6] European Civil Aviation Conference ECAC.CEAC Doc29 (3rd edition, 2005): Report on standard method of computing noise contours around civil airports. Volume 1: Applications guide, Volume 2: Technical guide.

[7] I. L. N. Granoien, R. T. Randberg: Corrective measures for aircraft noise models, new algorithms for lateral attenuation. Joint Baltic-Nordic Acoustics Meeting, Mariehamn, Aland, 8-10 June 2004, www.acoustics.hut.fi/ asf/ bnam04/ webprosari/ papers/ o41.

[8] W. Krebs, R. Bütikofer, S. Plüss, G. Thomann: Modelling of three-dimensional sound directivity patterns of helicopters. Acta Acustica united with Acustica **89** (2003) 273–279.

[9] W. Krebs, R. Bütikofer, S. Plüss, G. Thomann: Spectral three-dimensional sound directivity models for fixed wing aircraft. Acta Acustica united with Acustica **92** (2006) 269–277.

[10] ISO 9613-1: Acoustics - Attenuation of sound during propagation outdoors. Part 1: Calculation of the absorption of sound by the atmosphere. International Organization for Standardization, Switzerland, 1993.

[11] I. U.: On the reflection if a spherical sound wave from an infinite plane. J. Acoust. Soc. Am. **23** (1951) 329–335.

[12] R. B. Lawhead, I. Rudnick: Acoustic wave propagation along a constant normal impedance boundary. J. Acoust. Soc. Am. **23** (1951) 546–549.

[13] C. F. Chien, W. W. Soroka: Sound propagation along an impedance plane. J. Sound Vib. **43** (1975) 9–20.

[14] T. W. F. Embleton, J. E. Piercy, N. Olson: Outdoor sound propagation over ground of finite impedance. J. Acoust. Soc. Am. **59** (1975) 267–277.

[15] R. J. Donato: Propagation of a spherical wave near a plane boundary with a complex impedance. J. Acoust. Soc. Am. **60** (1976) 34–39.

[16] M. E. Delany, E. N. Bazley: Acoustical properties of fibrous absorbent materials. Applied Acoustics **3** (1970) 105–116.

[17] C. I. Chessell: Propagation of noise along a finite impedance boundary. J. Acoust. Soc. Am. **62** (1977) 825–834.

[18] K. Attenborough, S. I. Hayek, J. M. Lawther: Propagation of sound over porous half-space. J. Acoust. Soc. Am. **68** (1980) 1493–1501.

[19] P. Boulanger, T. Waters-Fuller, K. Attenborough, K. M. Li: Models and measurements of sound propagation from a point source over mixed impedance ground. J. Acoust. Soc. Am. **102** (1997) 1432–1442.

[20] Nordic Noise Group: Nordic outdoor propagation models for a homogeneous atmosphere. DELTA Acoustics & Vibration, AV 942/97, 70-80, 1997.

[21] K. M. Li, S. Taherzadeh, K. Attenborough: Models and measurements of sound propagation from a point source over mixed impedance ground. J. Acoust. Soc. Am. **101** (1997) 3343–3352.

[22] K. M. Li, M. Buret, K. Attenborough: The propagation of sound due to a source moving at high speed in a refracting medium. Proc. Euronoise 98, München, 1998, 955–960.

[23] M. Buret, K. M. Li, K. Attenborough: Optimisation of ground attenuation for moving sound sources. Appl. Acoust. **76** (145-156) 2006.

[24] E. Salomons: Computational atmospheric acoustics. Kluwer, The Netherlands, 2001.

[25] Society of Automotive Engineers: Procedure for the computation of airplane noise in the vicinity of airports. SAE 1845, 1986.

[26] J. M. Gulding, J. R. Olmstead, G. G. Fleming: Integrated noise model (INM), Version 6.0, User's guide. Federal Aviation Administration (FAA), Department of Transportation, Report No FAA-AEE-99-03, September 1999.

[27] S. Pietrzko, R. F. Hofmann: Prediction of A-weighted aircraft noise based on measured directivity patterns. Appl. Acoust. **23** (1988) 29–44.

[28] AzB - Der Bundesminister des Inneren: Anleitung zur Berechnung von Lärmschutzbereichen an zivilen und militärischen Flughäfen nach dem Gesetz zum Schutz gegen Fluglärm vom 30.3.1971. GMBI 26, Ausg. A, Nr. 8, 162-227, Bonn, 10. März 1975.

[29] DIN 45'684-1: Ermittlung von Fluggeräuschimmissionen an Landeplätzen. Teil 1: Berechnungsverfahren. 2006-09.

[30] FLULA2: Technical program documentation, Vers. 2.1. Empa, 2005.

[31] W. Krebs, R. Bütikofer, S. Plüss, G. Thomann: Sound source data for aircraft noise simulation. Acta Acustica united with Acustica **90** (2004) 91–100.

[32] EN 61672-1: Electroacoustics - Sound level meters - Part 1: Specifications. IEC 61672-1:2002.

[33] O. Zaporozhets, V. Tokarev, K. Attenborough: Prediction noise from aircraft operated on the ground. Appl. Acoust. **64** (941-953) 2003.